JOURNAL OF PHYSICAL ORGANIC CHEMISTRY
*J. Phys. Org. Chem.* 2003; **16:** 475–483
Published online in Wiley InterScience (www.interscience.wiley.com). DOI: 10.1002/poc.610

# *Ab initio* molecular dynamics studies on substitution vs electron transfer reactions of substituted ketyl radical anions with chloroalkanes: how do the two products form in a borderline mechanism?

**Hiroshi Yamataka,[1]* Misako Aida[2]* and Michel Dupuis[3]***

[1]Institute of Scientific and Industrial Research, Osaka University, Ibaraki, Osaka 567-0047, Japan
[2]Faculty of Science, Hiroshima University, Kagamiyama, Higashi-Hiroshima 739-8526, Japan
[3]Pacific Northwest National Laboratory, EMLS/K1-83, Battelle Blvd, Richland, Washington 99352, USA

*Received 8 October 2002; revised 22 November 2002; accepted 2 December 2002*

ABSTRACT: We present a qualitative analysis, based on *ab initio* molecular dynamics (MD) calculations, of the $S_N2$/ET mechanistic spectrum for three reactions: (1) $HC(CN)=O^{\bullet -} + CH_3Cl$, (2) $HC(CN)=O^{\bullet -} + (CH_3)_2CHCl$ and (3) $H_2C=O^{\bullet -} + CH_3Cl$, passing through their $S_N2$-like transition states. Finite temperature (298 K) direct MD simulations indicate that the trajectories for reaction (1) appear to have a propensity towards $S_N2$ products, the propensity for trajectories for reaction (2) seems to be towards ET products, whereas trajectories for reaction (3) appear to show no particular propensity towards either ET or $S_N2$ products. The mechanistic diversity is consistent with the electron-donating ability of the ketyl species and steric bulkiness of chloroalkanes. We find that the trajectories have characteristics that reflect strongly the types of process [$S_N2$ trajectories in reactions (1) and (3) vs ET trajectories in reactions (2) and (3)]. Trajectories that lead to $S_N2$ products are simple with C—C bond formation and C—Cl bond breaking essentially completed within 50 fs. By contrast, trajectories leading to ET products are more complex with a sudden electron reorganization taking place within 15–30 fs and the major bonding changes and electron and spin reorganizations completed after 250 fs. Copyright © 2003 John Wiley & Sons, Ltd.

KEYWORDS: direct molecular dynamics simulation; MO calculations; borderline mechanism; electron transfer; $S_N2$; transition state

## INTRODUCTION

An organic reaction that proceeds via an intermediate mechanistic region between two extremes is called a borderline reaction. Aliphatic nucleophilic substitution reactions are one such example: the substitution of a primary substrate occurs via an $S_N2$ mechanism whereas a tertiary substrate reacts through an $S_N1$ mechanism, while reactions involving secondary substrates, such as isopropyl halide, proceed with intermediate mechanistic characteristics (see, e.g., Ref. 1). Electron transfer (ET) reactions and polar nucleophilic substitutions have also borderline mechanistic regions depending on the donor/acceptor combination (for mechanistic crossover for $S_N2$/ET dichotomy, see Ref. 2). The experimental study by Kimura and Takamuku (Scheme 1) on an intramolecular reaction of carbonyl radical anion and haloalkane provides an example of such $S_N2$/ET borderline reactions.[3] Here the radical anions of 1-benzoyl-$\omega$-haloalkanes generated by pulse radiolysis gives two different products; one is characterized as an ET product and the other as an $S_N2$ product. The product ratio varies with the methylene chain length, the identity of the halogen leaving group, and the solvent. An interesting observa-

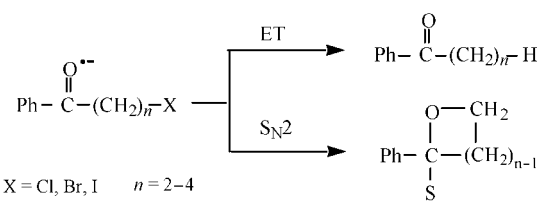


**Scheme 1**

**Correspondence to:* H. Yamataka, Institute of Scientific and Industrial Research, Osaka University, Ibaraki, Osaka 567-0047, Japan.
E-mail: yamataka@sanken.osaka-u.ac.jp
M. Aida, Faculty of Science, Hiroshima University, Kagamiyama, Higashi-Hiroshima 739-8526, Japan.
E-mail: maida@hiroshima-u.ac.jp
M. Dupuis, Pacific Northwest National Laboratory, EMLS/K1-83, Battelle Blvd, Richland, Washington 99352, USA.
E-mail: michel.dupuis@pnl.gov
*Contract/grant sponsor:* Ministry of Education, Science, Sports and Culture, Japan.

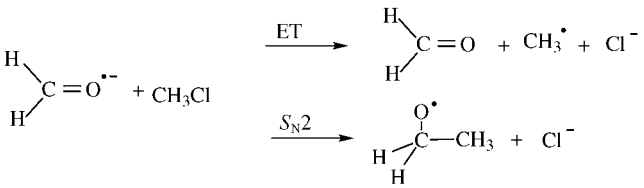


**Scheme 2**

tion regarding these reactions is that the rate of the product formation is identical for the two products and correlates well with the reduction potential of the substrate, whereas no simple linear relation exists between the rate of the reaction and the product ratio.

The analysis of the mechanism of borderline reactions is not straightforward. There are several experimental criteria[1] that can be used to assign the mechanism, but all of these criteria simply show that borderline reactions exhibit intermediate character between the two extremes. Hence the answer to the mechanistic problem is difficult to obtain through experimental studies that give only a macroscopic picture of the reaction, i.e. an average of microscopic events. The reaction may proceed via two concurrent routes, $S_N2$ and $S_N1$, or $S_N2$ and ET, and the experimental observation is an average of such independent processes. As for $S_N2$/ET borderline cases, there is computational evidence that two types of transition states (TS) exist: $S_N$-like TSs and ET-like TSs.[4] The relative energy between these two types of TS varies with the size and type of the substituent groups and with the halogen, and the energy differences can be very substantial (up to 1 eV).[4b] Very importantly, however, the $S_N$-like and ET-like TSs appear to lie in very distinct parts of phase space.[4b] Additionally, there is much computational evidence that the $S_N$-like TS appears to be of 'intermediate' character and appears to lead to both $S_N$ products and ET products.[4–7] A question arises then as to how the two different types of products are formed through the single $S_N$-like TS of intermediate character.

*Ab initio* MO calculations of $S_N2$/ET bifurcation in the formaldehyde radical anion and methyl chloride system (Scheme 2) have been reported by two groups.[4,5] Two pathways are envisaged: an $S_N2$ mechanism involving the carbonyl carbon atom to give the *C*-substitution product directly, and an ET mechanism to give neutral aldehyde, $CH_3$ radical and $Cl^-$, which eventually gives the C-substitution product. One well-characterized TS structure of $S_N2$ character was obtained, as shown in Fig. 1 (3), with the reaction coordinate consisting of an asymmetric C—C—Cl stretching motion. An intrinsic reaction coordinate (IRC) analysis by Bertran *et al.*[4] indicated that the TS was connected to the *C*-substituted $S_N2$ product. Shaik and co-workers[5a,c] reported that the steepest descent path connects the TS to the ET product. In Shaik and co-workers' work the origin of the different mechanistic assignment for the TS was analyzed on the basis of the potential energy surface at the UHF/6–31G* and ROHF/6–31G* levels of theory.[5c,d] They observed that the reaction path descends from a broad saddle point to a flat ridge that separates the $S_N2$ and ET products. After entering the flat ridge region, the path bifurcates to the two product states.[5] Although another TS structure of ET character exists,[4] that lies noticeably in a very distinct part of phase space, the fact remains that the $S_N2$-like TS yields to a bifurcating behavior.[4,5,7]

Shaik *et al.* also reported that the reactions of a series of chloroalkanes with cyanoformaldehyde radical anion belonged to an $S_N2$/ET mechanistic spectrum (Scheme 3).[5c] The reaction of cyanoformaldehyde radical anion and $CH_3Cl$ or $CH_3CH_2Cl$ gave the $S_N2$ products, whereas the same radical anion yielded the ET products with $(CH_3)_2CHCl$ and $(CH_3)_3CCl$, and thus a mechanistic changeover occurred between reactions with $CH_3CH_2Cl$ and $(CH_3)_2CHCl$. Another series of reactions of HYC═O radical anions with $CH_3X$ (Y = H, $CH_3$, CN; X = Cl, Br, I) again showed that the mechanism changed from $S_N2$ to ET depending on the donor/acceptor combinations.[5e] Overall, the reactions of aldehyde radical anions with haloalkanes constitute an $S_N2$/ET mechanistic spectrum with a borderline region between the two mechanistic extremes.

The analysis of the electronic structural character of the reactive system during the course of a reaction, in particular borderline reactions, represents a challenge. Charge and spin transfer and localization change with the molecular structure along the reaction pathway. In turn, these electronic effects are what determine the forces on the atoms and thus the reaction pathway and mechanism. In addition, the electronic structure of the reacting solute and its energy are affected by the finite temperature motion of the solvent molecules and the energy exchange between the solute and the solvent. Thus, the true mechanistic assignment ought to be done on the basis of finite temperature dynamics rather than of 0 K dynamics.[5c,d,6] Such dynamics calculations should be carried out on quantum mechanical potential energy surfaces, for example using the HF/6–31G* level of theory or higher levels, ideally with an explicit account of solvent molecules. This is the approach that we used in the present study.

We and others have reported earlier on *ab initio* molecular dynamics (MD) simulations[7] on the prototypical borderline $S_N2$/ET reaction of the formaldehyde radical anion with methyl chloride. One of the observations from this earlier study was that the finite temperature simulations yield both types of products.[4,5] The ET/$S_N2$ dichotomy through the $S_N2$-like TS is not an artifact of the IRC vs steepest descent path characterization. Here we have extended this work to a broader set of systems. We report the results of MD simulations for three substituted analog reactions of $HYC{=}O^{\bullet -} + RCl$ with (1) Y = CN, R = $CH_3$, (2) Y = CN, R = $(CH_3)_2CH$ and (3) Y = H, R = $CH_3$, and analyze the effect of substituents and of the temperature. In *ab initio* direct MD calculations, the energies and forces of the system at

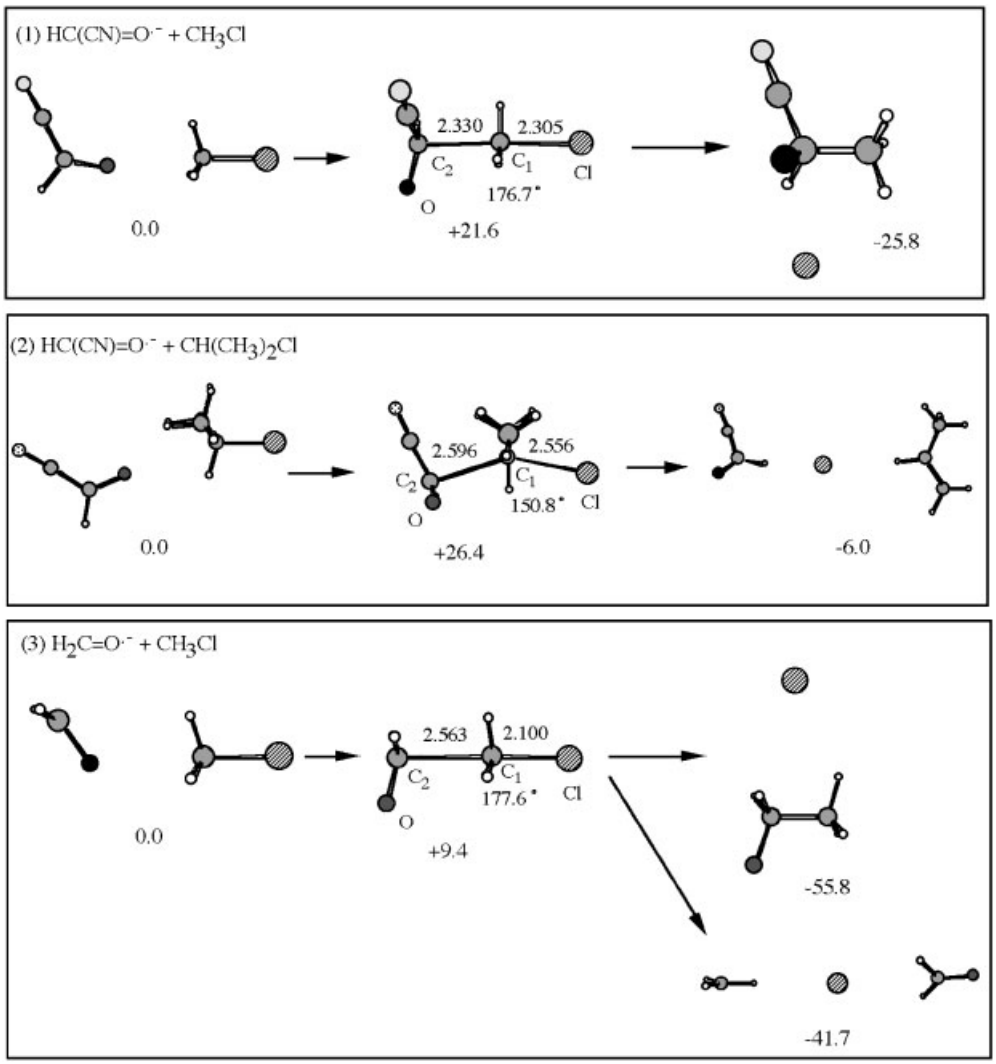


**Figure 1.** Stationary structures (reactant complex, TS and product complex) optimized at the HF/6–31+G* level for reactions (1)–(3) and selected geometric parameters of the TS structures. Atomic distances in Å and bond angles in degrees. Numbers given below the structures are energies (kcal mol$^{-1}$) relative to the reactant complexes

each time step are computed by a given *ab initio* MO method and the forces are used to solve Newton's equation of motion. The reliability of the MD simulations (and for that matter also of IRC analyses) depends very much on the qualitative and quantitative descriptions of the forces. The MD simulations differ from MO-based calculations in that the MD simulations give a dynamic picture of chemical reactions at a given temperature, in contrast to the zero-kinetic energy and classical picture provided by MO calculations of an IRC. *Ab initio* MD simulations are still expensive at the present stage of computational capability, and it is a challenge to perform such studies to analyze mechanistic problems that can not be approached by other means.[8,9] The key issues that we addressed in the present study are: (i) whether the $S_N2$ and ET products are formed mutually exclusively or not via the common $S_N2$-like TS structure in the borderline reaction and (ii) how the trajectories in the borderline region differ from those in the extreme regions ($S_N2$ products only and ET products only).

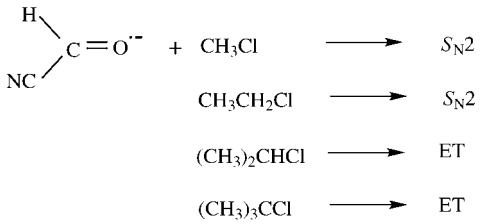


**Scheme 3**

The process of switching over from an $S_N2$-like to an ET-like product during the course of a single trajectory is suggestive of two quasi-diabatic surfaces coming close together in the region of the cross-over, one for the $S_N2$ product and the other for the ET product. The proximity of these two surfaces suggests that the reactive system

may undergo one or several non-adiabatic excursions on to an ET surface during the reaction on the lower $S_N2$ surface before falling into either of the product channels. The occurrence of such excursions may have significant qualitative and quantitative effects on branching mechanisms and branching ratios. A complete dynamic description of reactions with non-adiabatic excursions would require a treatment by means of non-adiabatic trajectory methods.[10] Such a treatment is not included here, albeit it should be the subject of further investigations. It would be interesting to see how much non-adiabatic excursions would alter the qualitative character of the trajectories described below. It is noticeable that the ET 'transition states' determined in Ref. 4b show an energy cusp traditionally associated with non-adiabatic processes. Non-adiabatic effects are likely to be even more important in these regions of phase space. The present study did not include non-adiabatic effects and can serve as a starting picture for more complete treatments in the future.

## COMPUTATIONAL METHODS

The classical nuclear trajectories were integrated from the energy and forces calculated by the MO method using a fourth-order Gear predictor–corrector algorithm,[11] and time steps of 0.5 fs were used (unless noted otherwise) to insure numerical accuracy, in particular in dealing with the high-frequency vibrational motions (CH stretches). We adopted a velocity re-scaling algorithm similar to the constant-temperature algorithm of Berendsen *et al.*[12] to mimic the solvent effects. These authors devised their algorithm to model the solute–solvent thermal exchange in an equilibrium solvation regime. They suggested a solute–solvent relaxation time of $\tau = 50$ fs as a mid-range value. In the present situation the system is in a non-equilibrium solvation regime, with the kinetic energy of the system quenched by the solvent as the system evolves down the reaction path. In a study that presents some similarities with the present work, of the relaxation dynamics of electronically excited formaldehyde in water, Levy *et al.*[13] reported that the formaldehyde solute cools at a rate of $\sim$7 kcal mol$^{-1}$ (1 kcal = 4.184 kJ) per picosecond, early during the relaxation. We carried out preliminary calculations that indicated that a similar cooling rate for the system at hand is obtained with a relaxation time $\tau \approx 2000$ fs using the velocity re-scaling algorithm of Berendsen *et al.*[12] We view such an algorithm as providing a reasonable and required mimic of solvent quenching for this reactive system.

All simulations were started from the given TS structures with initial velocities for each atom randomly generated according to a Maxwell–Boltzmann distribution, with the total kinetic energy of the system consistent with the simulation temperature. The proper treatment of the quantization of the nuclear vibrations in dynamics simulations continues to be a challenge.[14] In correct treatments of chemical dynamics the trajectories should maintain (possibly varying) quanta of vibrational energy (possibly zero-point energy) in the vibrational modes, starting with the initial conditions.[15] However, classical dynamics loses track of the vibrational quantization as soon as the trajectory is started, and it is often found that too much of the ZPE energy (over 40 kcal mol$^{-1}$ for the ketyl anion + chloromethane system) flows from the transverse modes into the reaction mode of the system, leading to unrealistic dynamics. A commonly used approach for large systems is to assign initially the atoms with a Maxwell–Boltzmann distribution of velocities. By assigning only a small amount of kinetic energy to any and all modes, a Maxwell–Boltzmann distribution of velocities yields a narrower range of motions than do distributions accounting for the zero-point energies in the modes. For stiff modes the thermal energy is much less than the ZPE of each of these stiff modes, and therefore the systems vibrates only very slightly along these modes. For the soft modes that in fact are not harmonic in character, it is appropriate to assign them a thermal amount of vibrational energy. Overall the initial vibrational energy resulting from a Maxwell–Boltzmann distribution consistent with a 300 K temperature is small enough that there is essentially no opportunity for the vibrational energy to flow excessively into the reactive mode or any other mode. Stiff modes are treated as if the atoms stayed around the equilibrium position in these modes on average, whereas the soft modes with large amplitude are provided the opportunity to have a wide range of motions. For these reasons, the simulations carried out for this study were based on Maxwell–Bolzmann distribution of the random initial atomic velocities. We believe that this is the most appropriate choice for the qualitative characterization that we seek, in contrast to a quantitative calculation of rates and branching ratios.

We performed 10 simulations for reactions (1) and (2) and 51 simulations for reaction (3) at 298 K in order to see whether the given TS leads to the $S_N2$ or ET product for each reaction system. The same numbers of trajectories were also calculated at different temperatures (100 and 400 K) to see the effect of the reaction temperature. The MO calculations were carried out at the UHF/6–31 + G* level of theory, unless noted otherwise. Diffuse functions were included in the basis set because of the anionic species. This basis set was shown to give reasonable results both in geometry and relative energy for the species under consideration here.[5b] The ROHF/6–31 + G* and CASSCF/6–31 + G* methods were also used for reaction (3). These levels of theory are sufficient to obtain qualitatively reliable descriptions of the classical reaction dynamics. The CASSCF method includes all the electron configurations, including spin-recoupling configurations, and better describes bond breaking and bond formation.

The limited number of trajectories calculated does not permit us to quantify branching ratios in any way. However, we are in a position to observe common qualitative features among the trajectories. Some of the simulations were also repeated at 50 and 10 K for reaction (3). In all reactions, the simulations moved either toward the reactant state or the product state, and only representative results are shown in this paper because the trajectories are essentially the same when they go to the same product type. Finally, it is possible that some of the trajectories may have crossed and/or re-crossed the transition state region, or crossed over from one bifurcating path to the other path down the reaction trajectories, as occurs in reality. We did not attempt to characterize such phenomena. Quantification of reaction rates and branching ratios would account for these processes. They are beyond the scope of this work, since we are not in a position to carry out such a quantification, owing to the limited number of trajectories. The program package of HONDO 2002 was used for the *ab initio* MD calculations.[16]

## RESULTS AND DISCUSSION

### MO calculations

The stationary structures determined by the *ab initio* MO calculations at the UHF/6–31 + G* level are summarized in Fig. 1. The stationary structures were reoptimized starting from the structures at similar levels reported in the literature.[5b,d] The MO calculations were carried out by using the Gaussian 94 suite of programs.[17] In all cases the reactant complexes show some interaction between the aldehyde oxygen and the carbon reaction center. The TSs are 9–26 kcal $mol^{-1}$ higher in energy than the reactant complexes. The barrier is higher for the HC(CN)=O radical anion since this species is more stable and a weaker nucleophile (electron donor) than the $H_2C$=O radical anion. All three TS structures have characteristics of $S_N2$ reactions, with the asymmetric motion of the C—C—Cl unit dominating the reaction coordinate. The TS for reaction (2) is looser than that for reaction (1) and the C—C—Cl angle differs from 180° owing to steric effects. The TS for reaction (3) is more reactant-like than that for reaction (1), in accord with Hammond's postulate.[18]

**$HC(CN)=O^{\bullet -} + CH_3Cl$.** Ten trajectories were generated starting from the TS structure of reaction (1) with random initial velocities at 298 K. It was found that three of the trajectories went to the reactant state, and seven reached the product state. Figure 2 contains the results of one of the simulations that lead to the product state. The changes in the potential energy [Fig. 2(a)] and in the C—Cl, C—C and C—O bond lengths [Fig. 2(b)] for 400 fs indicate that the C—C bond formation and the C—Cl bond breaking occur in a concerted manner soon after the system leaves the TS. The substitution is essentially completed within 40–50 fs and the $H(CN)CCH_3O$ radical and the chloride anion move away thereafter. The snapshot structure obtained after 400 fs shown in Fig. 3(a) clearly illustrates that the TS leads to the substitution product. Thus, the result of the dynamics simulation agrees with the MO calculations, in that the TS is connected to the $S_N2$ product state. Changes in charge and spin density are consistent with the $S_N2$ process: a unit charge appears on $Cl^-$ and a unit spin density on the carbonyl oxygen.

**$HC(CN)C=O^{\bullet -} + (CH_3)_2CHCl$.** The mechanistic assignment from the MO calculations for this reaction suggested that the reaction may fall in a borderline region (the steepest descent path connects the TS to the ET product whereas the IRC leads to the $S_N2$ product, just like the reaction of $H_2C$=O radical anion with $CH_3Cl$).[5d] In the present MD study, some of the trajectories were observed to go backwards to the reactant state while others went forward to the product state. At 298 K, all forward trajectories reached the ET product. The snapshot structure [Fig. 3(b)] obtained after 400 fs in one of

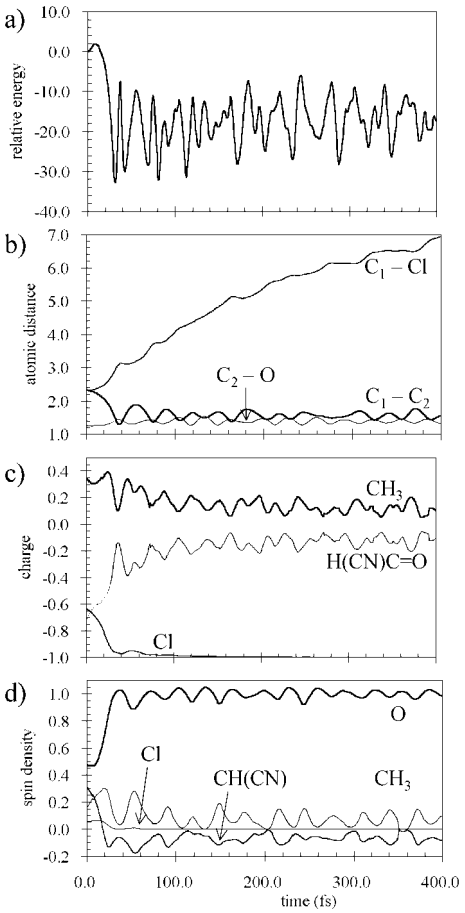


**Figure 2.** Trajectory leading to the product state for reaction (1) [$HC(CN)=O^{\cdot -} + CH_3Cl$]. (a) Potential energy (kcal $mol^{-1}$); (b) atomic distances (Å); (c) Mulliken group charge; and (d) spin density

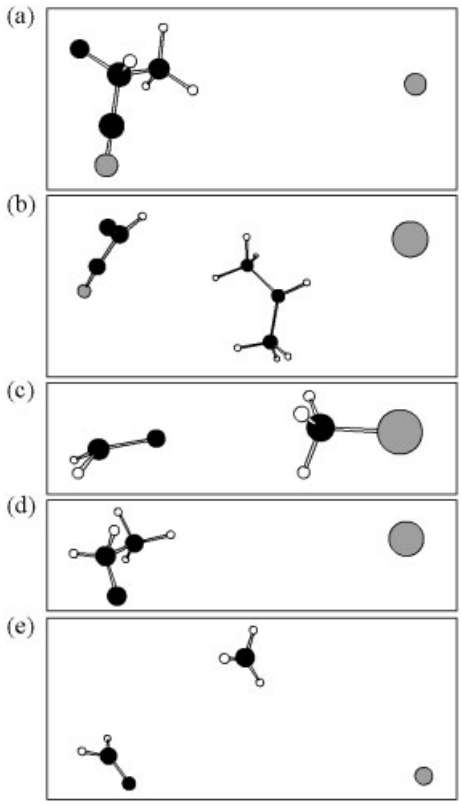


**Figure 3.** Snapshot structures obtained by simulations (a) for reaction (1) [HC(CN)═O$^{\cdot -}$ + $CH_3Cl$] after 400 fs leading to the $S_N2$ product, (b) for reaction (2) [HC(CN)═O$^{\cdot -}$ + $(CH_3)_2CHCl$] after 400 fs leading to the ET product, (c) for reaction (3) ($H_2C$═O$^{\cdot -}$ + $CH_3Cl$) after 100 fs leading to the reactant state with time step of 0.5 fs, (d) for reaction (3) after 400 fs leading to the $S_N2$ product and (e) for reaction (3) after 400 fs leading to the ET product

these trajectories clearly shows that this is the ET process. On the other hand, at the lower temperature (100 K) trajectories gave the $S_N2$ rather than ET product. In spite of the limited number of trajectories calculated, we interpret this finding as an example of mechanistic changeover with temperature.

Figure 4 shows the results of one trajectory starting from the TS of reaction 2 at 298 K. It is observed that along the trajectory the C—Cl bond breaks while the C—C bond length becomes short during the earlier phases of the reaction and then larger during the later phases. The variation of the C—C bond length is consistent with the recoil mechanism proposed by Shaik and co-workers[5b–d] on the basis of their path-following analysis. Because there is a considerable interaction between the formaldehyde carbon and the reaction carbon center in this 'bound' ET TS[6] and also because the reaction-coordinate vibration consists of the C—C bond formation together with the C—Cl bond breaking mode, it is reasonable to expect that the C—C bond becomes short at the early stage of the trajectory. Then, as the reaction proceeds, the two carbons start to separate due to a larger steric interaction and the higher radical stability of the isopropyl group. Thus, the driving forces to form the C—C bond are weaker for this reaction system than for reaction (1). As the reaction proceeds, the charge on the aldehyde group becomes zero and a unit charge becomes localized to form the chloride ion, $Cl^-$. A unit spin density moves from the aldehyde moiety to the $(CH_3)_2CH$ group. Although it takes nearly 200 fs for the overall reaction to complete, the charge and spin reorganizations occur at an early stage of the reaction within 10–15 fs. This rapid electronic reorganization is a manifestation of an electron transfer event during the reaction. After the electron reorganization, the spin density on Cl stays constant near zero whereas on $(CH_3)_2CH$ it varies from 0.80 to 1.00. The variations of the spin density on the HC(CN)═O substructure are noticeable, the total spin density nearly equals zero, yet the $\alpha$ and $\beta$ spins tend to separate, one on CHCN moiety and the other on O atom, akin to a diradical character within the molecule. This implies that an orbital interaction exists between the isopropyl carbon and the carbonyl carbon during the time span in which the two

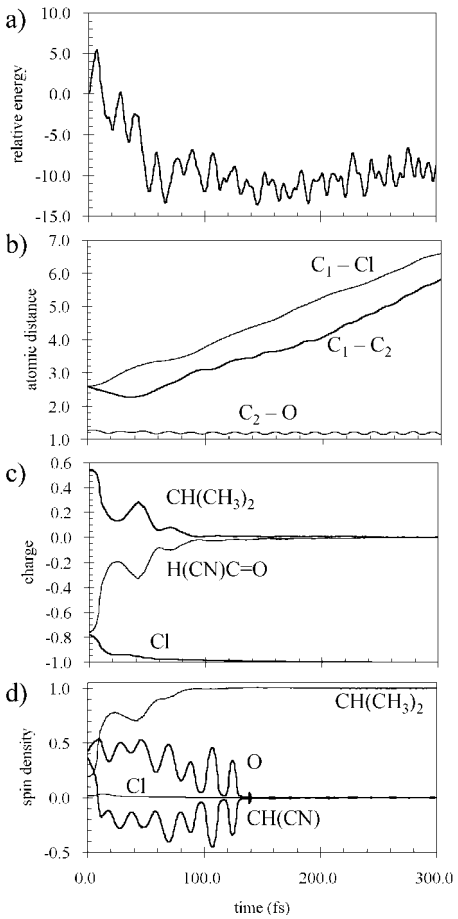


**Figure 4.** Trajectory leading to the product state for reaction (2) [HC(CN)═O$^{\cdot -}$ + $(CH_3)_2CHCl$]. (a) Potential energy (kcal mol$^{-1}$); (b) atomic distances (Å); (c) Mulliken group charge; and (d) spin density

fragments stay close together. Such spin separation diminishes when the C—C atomic distance becomes 3.5 Å or larger. It is seen that the spin densities on the aldehyde moiety oscillate with a period of about 20 fs, in perfect synchronism with the C—O stretching period. Indeed, 20 fs corresponds roughly to a frequency of 1700 $cm^{-1}$ of a carbonyl bond-stretching vibration.

**$H_2C{=}O^{\bullet -} + CH_3Cl$.** The *ab initio* MD simulations on borderline reaction (3) generated trajectories that, starting from the TS, moved toward three different states. At 298 K, out of 51 trajectories calculated, 36 trajectories went to the $S_N2$ product state and three led directly to the ET product state in addition to 12 trajectories that went back to the reactant state. It is interesting that four out of 36 trajectories toward $S_N2$ went over to the ET product state after staying some time in the $S_N2$ valley. This turnover process is apparently due to excess energy residing in the C—C stretching mode after the trajectory reached the $S_N2$ valley.[7c] Snapshot structures obtained after 400 fs of $S_N2$ and ET trajectories are shown in Fig. 3(d) and (e), respectively.

The trajectory leading to the reactant state is a simple one, in which $CH_3Cl$ and formaldehyde radical anion are generated in 30 fs. The fluctuations observed in the C—Cl distance and the group charges have a periodicity of about 50 fs, which corresponds to ca 670 $cm^{-1}$ of the C—Cl stretching vibration.[20] The frequency of the potential energy fluctuation is twice of that of the C—Cl distance because the potential energy goes through a minimum twice per each stretching vibration. The snapshot structure obtained after 100 fs [Fig. 3(c)] is similar in nature to the reactant complex determined in the MO calculations (0 K) (Fig. 1), with the interaction of the carbonyl oxygen with the methyl carbon being the major interaction between the two fragments.

One of the trajectories that go to the $S_N2$ product is shown in Fig. 5. The trajectory looks remarkably similar to that observed for the $S_N2$ process of reaction (1) (Fig. 2). This finding indicates that, at least in the present system, the $S_N2$ reaction pathway in a borderline mechanism is similar to a plain $S_N2$ pathway, although the TS lies earlier on the reaction path for the borderline reaction. The only difference between the two trajectories is seen in the variation of the spin density on the $CH_3$ group, which appears for reaction (3). This may be due to a stronger ET character for the borderline process [reaction (3)] than for the $S_N2$ process [reaction (1)].[19,20] The spin contamination is small ($<S^2> \approx 0.77$) at the TS, then it increases to a maximum of 0.88 at 40 fs, and decreases to ~0.76 at 50 fs. The time span of the trajectory matches the interval where rapid spin reorganization within $O{=}CH_2{—}CH_3$ occurs. The large spin contamination may cast some doubt on using the UHF method in the simulation. However, calculations using the CASSCF method gave nearly the same trajectory.

Figure 6 shows the one trajectory within the calculated set of trajectories that goes to the ET product. Here again the trajectory looks basically the same as that observed for a 'pure' ET process as in reaction (2). Thus the ET process in the borderline reaction has similar characteristics to the process of a pure ET mechanism. One difference is that the electron reorganization is sharper here in reaction (3) than in ET reaction (2). This difference may be related to the tighter TS and hence to the stronger interaction between the fragments in reaction (3) compared with reaction (2).

It is noticeable from the comparison of the $S_N2$ and ET trajectories of reaction (3) that the two classes of trajectories showed different characteristics in the variation patterns for the bond distances, group charges and spin densities, and this already immediately after the reaction moves away from the TS. For example, the C—C bond length decreases and the C—Cl bond length increases immediately after the trajectory starts to leave the TS in the $S_N2$ process, whereas both bonds increase only slightly for the first 30 fs and then start to change in the ET process. This difference indicates that the fate of the trajectories is determined by the crossing at the saddle point as a result of the initial random velocities of the

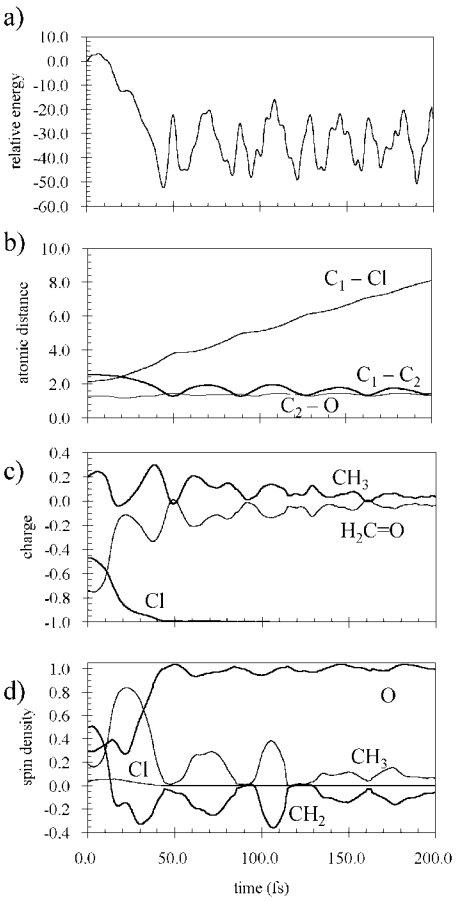


**Figure 5.** Trajectory leading to the $S_N2$ product state for reaction (3) ($H_2C{=}O^{\cdot -} + CH_3Cl$). (a) Potential energy (kcal $mol^{-1}$); (b) atomic distances (Å); (c) Mulliken group charge; and (d) spin density

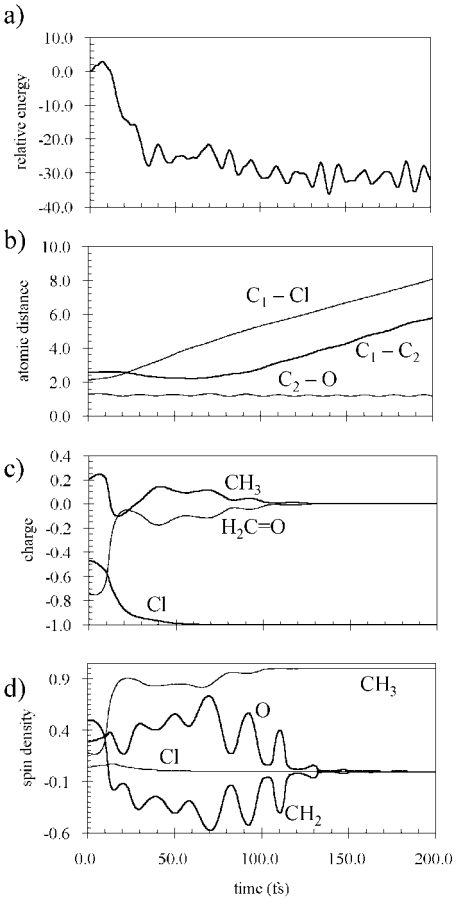


**Figure 6.** Trajectory leading to the ET product state for reaction (3) ($H_2C{=}O^{\cdot -} + CH_3Cl$). (a) Potential energy (kcal mol$^{-1}$); (b) atomic distances (Å); (c) Mulliken group charge; and (d) spin density

simulations. Although the reaction coordinate crosses the saddle point along the steepest descent path, it is only one of an infinite number of ways of passing the saddle point in a real reaction with sufficient thermal kinetic energy. This observation also supports the idea that mechanistic assignments by means of path-following analyses have limitations in borderline reactions.

**UHF vs ROHF simulations.** According to the potential energy mapping by Shaik and co-workers[5c,d] for reaction (3), the reaction path descends from a broad saddle point to a flat ridge that separates the $S_N2$ and ET products. On the UHF potential energy surface the steepest descent path is connected to the ET product state, whereas the IRC path leads to the $S_N2$ product state. In contrast, at the ROHF level of theory, the TS was shown to be connected to the ET product state on both the steepest descent path and the IRC path, and the TS was assigned as the ET TS.[5c,d] Since we found that trajectories from the TS lead dynamically to both the ET and $S_N2$ product states at UHF, it appeared informative also to carry out MD simulations on the ROHF potential energy surface. Thus, we repeated four simulations with ROHF as the MO part of the MD simulations, but using the same initial conditions as in the UHF cases. These were simulation 1 (ET product when using UHF), simulation 2 ($S_N2$ product when using UHF), simulation 3 ($S_N2$ product when using UHF) and simulation 4 (reactant state when using UHF). A detailed comparison of UHF and ROHF structures and energies for some of these systems was given by Sastry and Shaik.[5b] The structural parameters of the key structures at these levels of theories and, as found by us also with the CASSCF level of theory, were in good agreement with structures obtained with electron correlation theories such as MP2 and QCISD.

The simulations at the ROHF level of theory gave slightly different results from those at UHF. Specifically, simulation 2 turned out to now lead to the ET product state rather than to the $S_N2$ product. The products of the other three simulations turned out to be the same for both MO methods. The inclination toward the ET product state with the ROHF method is consistent with the difference in the potential energy surface arising from the two methods, i.e. the stronger spin coupling in the ROHF method. The important finding, however, is that even with the ROHF theory the single TS leads dynamically to both ET and $S_N2$ product states. Clearly, the MD trajectories with excess kinetic energy can overcome a small barrier on the way to the $S_N2$ product state. It should also be noted that, except for the fact that the spin separation detected in the ET trajectory at the UHF level (Fig. 6) does not occur at the ROHF level, the ET and $S_N2$ trajectories using ROHF are essentially the same as the corresponding trajectories using UHF.

**Trajectories at different temperatures.** Since the behavior of trajectories depends on the kinetic energy, it is of interest to carry out simulations at lower temperatures and to examine whether the trajectories in a lower temperature regime agree with the path-following results. As we have discussed in a preliminary report, trajectories at a lower temperature gave a higher propensity towards an ET process for reaction (3).[7c] A similar trend was found in the present study for reaction (2), which according to path-following calculations belongs to a borderline case. For this system, all trajectories that went to the product state at 298 K were of the ET type. However, at 100 K all these trajectories turned out to give the $S_N2$ state rather than ET. Clearly, the reaction mechanism changes with the amount of kinetic energy injected in these borderline systems. In contrast, reaction system (1) stayed $S_N2$ at all temperature examined, indicating that the mechanism of this reaction is purely $S_N2$.

## CONCLUSIONS

The present *ab initio* direct MD simulations on the

$S_N2$/ET processes show that reactions (1) [$HC(CN)=O^{\bullet -} + CH_3Cl$] and (2) [$HC(CN)=O^{\bullet -} + (CH_3)_2CHCl$] represent trajectories of $S_N2$ and ET processes, respectively, whereas the TS of reaction (3) ($H_2C=O^{\bullet -} + CH_3Cl$) is connected to both $S_N2$ and ET product states dynamically. The duality occurs because the fragmentation and vibrational energy allow for the reaction to proceed through a route away from the steepest descent path to overcome the ridge between the ET and $S_N2$ states. Such dynamic characteristics can only be treated by MD simulations based on quantum mechanical wavefunctions. The results are in accord with the idea that the TS characteristics alone are not sufficient to imprint the reaction mechanism, but that the thermal energy plays an important role. The formation of two different products does not necessarily imply the presence of two independent pathways with different TSs as is usually assumed in analyzing organic reaction mechanisms. The occurrence of branching from a single TS to several products introduces additional complexities in mechanistic assignment for borderline reactions.[21,22]

## Acknowledgements

The numerical calculations were carried out in part on the SP2 at the Research Center for Computational Science, Okazaki National Research Institute, Japan. This work was supported by a Grant-in-Aid for Scientific Research on Priority Areas 'Molecular Physical Chemistry' from the Ministry of Education, Science, Sports and Culture, Japan. The Pacific Northwest National Laboratory is a multiprogram national laboratory operated for the US Department of Energy by Battelle Memorial Institute under Contract DE-AC06-76RLO 1830.

## REFERENCES

1. Ingold CK. *Structure and Mechanism in Organic Chemistry* (2nd edn). Cornell University Press: Ithaca, NY, 1969; Lowry HT, Richardson KS. *Mechanism and Theory in Organic Chemistry* (3rd edn). Harper & Row: New York, 1987.
2. Daasbjerg K, Christensen TB. *Acta Chem. Scand.* 1995; **49**: 128–132; Daasbjerg K, Pedersen SU, Lunt H. *Acta Chem. Scand.* 1991; **45**: 424–430; Lunt H, Daasbjerg K, Lunt T, Pedersen SU. *Acc. Chem. Res.* 1995; **28**: 313; Savéant J-M. *Adv. Phys. Chem.* 1990; **26**: 1–130; Eberson L. *J. Chem. Soc., Chem. Commun.* 1975; 826–827; Lexa D, Savéant J-M, Su K-B, Wang D-L. *J. Am. Chem. Soc.* 1988; **110**: 7617–7625; Cho JK, Shaik SS. *J. Am. Chem. Soc.* 1991; **113**: 9890–9891; Herbert E, Mazaleyrat J-P, Welwart Z, Nadjo L, Savéant J-M. *Nouv. J. Chem.* 1985; **9**: 75–81; Daasbjerg K, Hansen JN, Lund H. *Acta Chem. Scand.* 1990; **44**: 711–714; Savéant J-M. *J. Am. Chem. Soc.* 1992; **114**: 10595–10602; Lund T, Lund H. *Acta Chem. Scand., Ser. B* 1986; **40**: 470–485; Lund T, Lund H. *Acta Chem. Scand., Ser. B* 1988; **42**: 269–279.
3. Kimura N, Takamuku S. *Bull. Chem. Soc. Jpn.* 1991; **64**: 2433–2437; *J. Am. Chem. Soc.* 1994; **116**: 4087–4088; see also Kimura N, Takamuku S. *Bull. Chem. Soc. Jpn*, 1993; **66**: 3613–3617; *J. Am. Chem. Soc.* 1995; **117**: 8023–8024.
4. (a) Bartran J, Gallardo I, Moreno M, Savéant J.-M. *J. Am. Chem. Soc.* 1996; **118**: 5737–5744; (b) Costentin C, Savéant J.-M. *J. Am. Chem. Soc.* 2000; **122**: 2329–2338.
5. (a) Sastry GN, Shaik S. *J. Am. Chem. Soc.* 1995; **117**: 3290–3291; (b) Sastry GN, Shaik S. *J. Phys. Chem.* 1996; **100**: 12241–12252; (c) Shaik S, Danovich D, Sastry GN, Ayala PY, Schlegel HB. *J. Am. Chem. Soc.* 1997; **119**: 9237–9245; (d) Sastry GN, Shaik S. *J. Am. Chem. Soc.* 1998; **120**: 2131–2145; (e) Sastry GN, Danovich D, Shaik S. *Angew. Chem., Int. Ed. Engl.* 1996; **35**: 1098–1100.
6. Zipse H. *Angew. Chem., Int. Ed. Engl.* 1997; **36**: 1697–1700.
7. (a) Yamataka H, Aida M, Dupuis M. *Chem. Phys. Lett.* 1999; **300**: 583–587; (b) Bakken V, Danovich D, Shaik S, Schlegel HB. *J. Am. Chem. Soc.*, 2001; **123**: 130–134; (c) Yamataka H, Aida M, Dupuis M. *Chem. Phys. Lett.* 2002; **353**: 310–316.
8. Aida M, Yamataka H, Dupuis M. *Chem. Phys. Lett.*, 1998; **292**: 474–480; Aida M, Yamataka H, Dupuis M. *Theor. Chem. Acc.* 1999; **102**: 262–271.
9. Chen W, Hase WL, Schlegel HB. *Chem. Phys. Lett.* 1994; **228**: 436; Li G, Hase WL. *J. Am. Chem. Soc.* 1999; **121**: 7124–7129.
10. Hammes-Schiffe, S, Tully JC. *J. Chem. Phys.* 1995; **103**: 8528–8537; Martinez TJ, Ben-Nun M, Levine RD. *J. Phys. Chem.* 1996; **100**: 7884–7895; Volobuev YL, Hack MD, Topaler MS, Truhlar DG. *J. Chem. Phys.* 2000; **112**: 9716–9726.
11. Allen MP, Tildesley DJ. *Computer Simulations of Liquids*. Oxford University Press: Oxford, 1987.
12. Berendsen HJC, Postma JPM, van Gunsteren WF, DiNola A, Haak JR. *J. Chem. Phys.* 1984; **81**: 3684–3690.
13. Levy RM, Kitchen DB, Blair JT, Krogh-Jespersen K. *J. Phys. Chem.* 1990; **94**: 4470–4476.
14. Stock G, Muller U. *J. Chem. Phys.* 1999; **111**: 65–76; Gio Y, Thompson DL, Sewell TD. *J. Chem. Phys.* 1996; **104**: 576–578; Peslherbe GH, Hase WL. *J. Chem. Phys.* 1994; **100**: 1179–1188; Sewell TD, Thompson DL, Gezelter JD, Miller WH. *Chem. Phys. Lett.* 1992; **193**: 512–517.
15. Peslherbe GH, Wang HB, Hase WL. *Adv. Chem. Phys.* 1999; **105**: 171–201.
16. Dupuis M, Marquez A, Davidson ER. HONDO 2002, based on HONDO96. Quantum Chemistry Program Exchange, Indiana University, 2002.
17. Frisch MJ, Trucks GW, Schlegel HB, Gill PMW, Johnson BG, Robb MA, Cheeseman JR, Keith T, Petersson GA, Montgomery JA, Raghavachari K, Al-Laham MA, Zakrzewski VG, Ortiz JV, Foresman JB, Cioslowski J, Stefanov BB, Nanayakkara A, Challacombe M, Peng CY, Ayala PY, Chen W, Wong MW, Andres JL, Replogle ES, Gomperts R, Martin RL, Fox DJ, Binkley JS, DeFrees DJ, Baker J, Stewart JP, Head-Gordon M, Gonzalez C, Pople JA. Gaussian 94. Gaussian: Pittsburgh, PA, 1995.
18. Hammond GS. *J. Am. Chem. Soc.* 1955; **77**: 334–338.
19. Pross A, Shaik SS. *Acc. Chem. Res.* 1983; **16**: 363–370
20. Pross A. *Adv. Phys. Org. Chem.* 1985; **21**: 99.
21. Carpenter BK. *Acc. Chem. Res.* 1992; **25**: 520–528.
22. Reys MB, Carpenters BK. *J. Am. Chem. Soc.* 1998; **120**: 1641, and references cited therein.